14th International Conference on Applications of Statistics and Probability in Civil Engineering, ICASP14
Dublin, Ireland, July 9-13, 2023

A Collaborative Bayesian Optimization Method for estimation of failure probability bounds under mixed uncertainties

Fangqi Hong
School of Power and Energy, Northwestern Polytechnical University, Xian, China

Pengfei Wei
School of Power and Energy, Northwestern Polytechnical University, Xian, China

Jingwen Song
School of Mechanical Engineering, Northwestern Polytechnical University, Xian, China

Marcos Valdebenito
Chair for Reliability Engineering, TU Dortmund University, Leonhard-Euler Strasse 5, 44227, Dortmund, Germany

Matthias Faes
Chair for Reliability Engineering, TU Dortmund University, Leonhard-Euler Strasse 5, 44227, Dortmund, Germany

Michael Beer
Institute for Risk and Reliability, Leibniz Universität Hannover, Hannover, Germany

ABSTRACT: Uncertainty quantification has been realized as of vital importance in structural reliability engineering to achieve credible results especially when the available information is scarce, incomplete, imprecise, etc., and it is also recognized that the aleatory and epistemic uncertainties need to be distinguished and separated and characterized through the whole analysis process. For addressing the above challenge, beyond the classical probability models, imprecise probability models, such as probability boxes, evidence theory, and fuzzy probabilities, as well as non-probabilistic models with interval/convex models as examples, have been developed for addressing alternative cases. However, given the mixed inputs characterized by the probability model, the imprecise probability, and the non-probabilistic model, the resultant failure probability is presented to be an interval variable, and it is then the key to estimating the bounds, especially the upper bound, of this interval. Following our development of Collaborative and Adaptive Bayesian Optimization for estimating the bounds of the expectation of the structural response, we propose a generalization of it for efficiently estimating the bounds of the failure probability by introducing several key improvements. The method starts by training a Gaussian Process Regression (GPR) model in the joint aleatory and epistemic spaces and then inferring the resultant stochastic process models in the marginal subspaces. With the above treatments, the double-loop formulation is then decoupled and two acquisition functions are introduced for specifying the optimal training points respectively in the two marginal spaces. Different from the original CABO algorithm, the above inference is realized based on an efficient numerical simulation of the GPR model, and thus applies to any output of interest. The above process is repeated until the stopping criteria are satisfied in both subspaces. Numerical results indicate that the CABO algorithm is efficient and shows good performance of global convergence.

1. INTRODUCTION

Quantifying alternative types of uncertainties and propagating them through expensive-to-estimate simulators have been realized as of vital importance in many research areas such as structural reliability engineering. It has also been realized that different types uncertainties need to be distinguished and separately characterized with proper mathematical models for making reliable estimation and decision on risk and reliability Abdar et al. (2021). Three groups of mathematical models, including probability model, imprecise probability models (such as probability boxes, evidence theory, and fuzzy probabilities) Beer et al. (2013) and non-probabilistic models (such as interval/convex models) Crespo et al. (2014) have been developed for addressing alternative scenario. Specifically, the probability model is most applied to the random parameters with sufficient information for characterizing the aleatory uncertainty; the imprecise probability models are applicable to random parameters with insufficient information for separately characterizing the aleatory and epistemic uncertainties; the non-probabilistic models are applied to the deterministic-but-unknown parameters for describing the epistemic uncertainty (see Crespo et al. (2014) for example). A major challenge in Uncertainty Quantification (UQ) is then the propagation of these three group of methods through the expensive-to-estimate simulators to quantifying the uncertainties of the outputs, and in this work, the estimation of the failure probability bounds, given the three kinds of uncertainty models as inputs, is of special concern.

Resulted from the hierarchical structure of the imprecise probability models, most available methods for addressing the above problem involves a double-loop scheme, and these methods follows two alternative strategies. The straightforward methods conduct the global optimization procedures in the space of epistemic uncertainty in the outer loop, then perform the probabilistic analysis, for examples, Monte Carlo Simulation (MCS) Raychaudhuri (2008), of the response of interest in the inner loop. The another strategy, called as Interval Monte Carlo Simulation (IMCS) Zhang et al. (2010), randomly create the random interval samples in the outer-loop, and carry out optimization methods to the response of interest in the inner-loop by performing either intrusive methods or non-intrusive methods Zhang et al. (2013). The above two strategies are utilized to address the 2014 NASA Langley UQ challenge problem Patelli et al. (2015). According to the structure of both strategies, computational burden maybe is heavy for computational expensive simulator as the required number of calling the time-consuming simulators is large for satisfying the required numerical errors.

For mitigating the computational cost cased by the double-loop procedure, many methods have been developed, such as, the decoupling methods Wei et al. (2014), and the surrogate model based methods, etc. Through, the decoupling methods can transform the double-loop scheme to a sing-loop scheme with the reduction the number of calling the model simulator, however, the computational burden is still too heavy to apply. The surrogate model based methods, such as Polynomial Chaos Expansion (PCE) Fox and Okten (2021), Neural Networks (NN) Abiodun et al. (2018), and Gaussian Process Regression (GPR) Rasmussen and Williams (2006), etc, build an easy-to-compute surrogate model replacing the computational expensive model response, and the corresponding probability analysis will be applied to the surrogate model for saving the computational cost. The prediction error of a GPR model is treated as a source of epistemic uncertainty, and is quantified by the posterior variance. The above property of GPR model is the most appealing character compared with other surrogate model methods, therefore, the GPR model is utilized in this paper.

For further improving the efficiency of estimating the bounds of variance and failure probability of an expensive simulator, the Bayesian Probabilistic Optimization (BPO) Hennig and Schuler (2012) and the stochastic simulation strategy Chiles and Delfiner (2009) are integrated in a collaborative and adaptive way and constitute a general Bayesian numerical framework to solve the optimization problems, which is inspired by CABO method Wei et al. (2021). The proposed frame-

work starts from a trained Gaussian process regression (GPR) model in the joint space of aleatory and epistemic uncertainty, and decouples the double-loop trap in a collaborative scheme, where the BPO is employed to optimize the global best points in the space of interval inputs and epistemic parameters, and the corresponding global optimal value is estimated by the Bayesian Probabilistic Integration (BPI) . Two learning functions are introduced to establish a adaptive deign strategy to collaboratively generate the optimal design points in the joint space of inputs and epistemic parameter. The proposed framework possesses several attractive characteristics, i.e., requiring few simulator calls, presenting quantification of numerical errors, applying to any kind of uncertainty characterization models, etc.

2. Problem Statements

Considering a deterministic model response of interest $y = g(x_I, x_{II}, x_{III})$, where $x_I = \left(x_I^1, \cdots, x_I^{n_I}\right)$ denotes the n_I-dimensional random input vector with its aleatory uncertainty characterized by a precise probability model $f_I(x_I)$ called probability density function, $x_{II} = \left(x_I^1, \cdots, x_{II}^{n_{II}}\right)$ represents the n_{II}-dimensional random input vector with $f_{II}(x_{II} \mid \theta)$ being the joint probability density function, where θ expresses the non-deterministic distributional parameter vector whose uncertainty modeled by the hyper-rectangle $\left[\theta^{\mathbf{L}}, \theta^{\mathbf{U}}\right]$, and $x_{III} = \left(x_{III}^1, \cdots, x_{III}^{n_{III}}\right)$ denotes n_{III}-dimensional interval input variables belonging to the hyper-rectangle $\left[x_{III}^{\mathbf{L}}, x_{III}^{\mathbf{U}}\right]$. The random uncertainty of the input variables (x_I, x_{II}, x_{III}) is characterized by probability density function $f_I(x_I)$ and $f_{II}(x_{II} \mid \theta)$, and the epistemic uncertainty of which is modeled by hyper-rectangular support $\left[x_{III}^{\mathbf{L}}, x_{III}^{\mathbf{U}}\right]$ and $\left[\theta^{\mathbf{L}}, \theta^{\mathbf{U}}\right]$. For simplicity, it is assumed that all input variables (x_I, x_{II}, x_{III}) are independent, the corresponding joint density and cumulative distribution function of (x_I, x_{II}) can be formulated as $f_I(x_I) = \prod_{i=1}^{n_I} f_I^i\left(x_I^i\right)$ and $f_{II}(x_{II}) = \prod_{i=1}^{n_{II}} f_{II}^i\left(x_{II}^i\right)$, where $f_I^i\left(x_I^i\right)$ and $f_{II}^i\left(x_{II}^i\right)$ represent the marginal density of x_I^i and x_{II}^i respectively.

Based on the above settings, the probabilistic characters of the g-function, such as statistical moments, are functions of the interval input vector x_{III} and the epistemic parameters θ. The target of this work is to estimate the bounds of these probabilistic characters, and specifically, the model output variance $V_y(x_{III}, \theta)$ and the failure probability $P_f(x_{III}, \theta)$, are of focus. These two characters are formulated as:

$$\begin{aligned} V_y(x_{III}, \theta) &= \int_{\mathbb{R}^{n_I + n_{II}}} \left(g(x_I, x_{II}, x_{III}) - m_y(x_{III}, \theta)\right)^2 \\ &\quad \times f_I(x_I) f_{II}(x_{II}|\theta) \, \mathrm{d}x_I \mathrm{d}x_{II} \\ P_f(x_{III}, \theta) &= \int_{\mathbb{R}^n} I_F(x_I, x_{II}, x_{III}) f_I(x_I) f_{II}(x_{II}|\theta) \, \mathrm{d}x_I \mathrm{d}x_{II} \end{aligned} \tag{1}$$

, where

$$\begin{aligned} m_y(x_{III}, \theta) = \int_{\mathbb{R}^n} & g(x_I, x_{II}, x_{III}) \\ & \times f_I(x_I) f_{II}(x_{II}|\theta) \, \mathrm{d}x_I \mathrm{d}x_{II} \end{aligned} \tag{2}$$

denotes the expectation function, $I_F(x_I, x_{II}, x_{III})$ indicates the indicators function of $g(x_I, x_{II}, x_{III})$ being less than zero, and is often called indicator function of the failure domain $F = \{(x_I, x_{II}, x_{III}) : g(x_I, x_{II}, x_{III}) < 0\}$. The bounds of the output variance and the probability of failure are then formulated as

$$\begin{cases} V_L = \min\limits_{\theta \in \left[\theta, \bar{\theta}\right], x_{III} \in [x_{III}, \bar{x}_{III}]} V_y(x_{III}, \theta) \\ V_U = \max\limits_{\theta \in \left[\theta, \bar{\theta}\right], x_{III} \in [x_{III}, \bar{x}_{III}]} V_y(x_{III}, \theta) \end{cases} \\ \begin{cases} P_{fL} = \min\limits_{\theta \in \left[\theta, \bar{\theta}\right], x_{III} \in [x_{III}, \bar{x}_{III}]} P_f(x_{III}, \theta) \\ P_{fU} = \max\limits_{\theta \in \left[\theta, \bar{\theta}\right], x_{III} \in [x_{III}, \bar{x}_{III}]} P_f(x_{III}, \theta) \end{cases} \tag{3}$$

For estimating the bounds of the output response m_y, the collaborative and adaptive Bayesian optimization (CABO) Wei et al. (2021) has been developed based on the properties of linear operation of the Gaussian process. However, this scheme cannot be directly extended to the response variance and the failure probability due to the non-linear mapping. In this work, we propose a efficient simulation scheme for realizing the extension.

3. Collaborative and adaptive Bayesian optimization framework

The estimation of the bounds of variance and failure probability of CABO involves a double-loop procedure. In the first-step, a Bayesian adaptive

optimization process is applied to search the minimum and maximum points of the variance or failure probability in the space of x_{III} and θ, and, an acquisition function is utilized to adaptively generate random design site to make the estimates satisfy the required estimated errors in the space of x_I and x_{II} in the second-step.

Before applying the procedure of CABO, the pretreatment is needed. First, the imprecise input variables x_{II} are need to be transformed to make it independent of θ by using $x_{II} = F_{II}^{-1}((u \mid \theta))$, where u follows independent uniform distribution in interval $[0,1]$, $F_{II}^{-1}((\cdot \mid \theta))$ is the inverse CDF of x_{II}. Then the g-function can be rewritten as $\mathscr{G}(\omega)$ in the augmented space $\omega = (x_I, u, x_{III}, \theta)$

Based on a set of training samples, a Gaussian process regression (GPR) model is trained in the space of ω, the specific procedures are introduced in the next subsection.

3.1. Gaussian process regression

Assume that $\mathscr{G}(\omega)$-function follows a Gaussian process $\mathscr{GP}(m(\omega), \kappa(\omega, \omega'))$ with $m(\omega)$ and $\kappa(\omega, \omega')$ being the prior mean function, and prior covariance function (kernel function). With no loss of generality, the exponential squared kernel function is applied in this paper, which is formulated as

$$\kappa(\omega, \omega') = \sigma_0^2 \exp\left(-\frac{(\omega - \omega')\Sigma^{-1}(\omega - \omega')^{\mathbf{T}}}{2}\right) \tag{4}$$

, where σ_0^2 and Σ indicate the hyper-parameters of the GPR model.

Let $D = (W, Y)$ denotes the training data set with size N_0, based of which, the hyper-parameters included in mean function and covariance function are then evaluated by maximizing the corresponding likelihood function of D. With all hyper-parameters estimated, the posterior Gaussian process $\hat{\mathscr{G}}_D(\mu_y(\omega), \mathrm{cov}_y(\omega, \omega'))$ can be derived with mean and covariance formulated as

$$\mu_y(\omega) = m(\omega) + \kappa(W, \omega)^{\mathbf{T}} K^{-1}(Y - m(W)) \tag{5}$$

and

$$\begin{aligned} \mathrm{cov}_y(\omega, \omega') =& \kappa(\omega, \omega') \\ & - \kappa(W, \omega)^{\mathbf{T}} K^{-1} \kappa(W, \omega') \end{aligned} \tag{6}$$

respectively, where $K = \kappa(W, W)$ denotes $N \times N$ matrix with the ij-th component K_{ij} being $\kappa(W_i, W_j)$, $\kappa(W, \omega)$ is N-dimensional column vector, the i-th component of which is $\kappa(W_i, \omega)$. It should be noted that the mean function of GPR model is the prediction at site ω, while the variance function measures the corresponding numerical error.

3.2. The adaptive optimization strategy

Once the GPR model $\hat{\mathscr{G}}_D(\omega)$ of $\mathscr{G}(\omega)$ is trained, the output variance function $V_y(x_{III}, \theta)$ and the failure probability function $P_f(x_{III}, \theta)$ can both be approximated by the induced stochastic processes $\hat{V}_y(x_{III}, \theta)$ and $\hat{P}_f(x_{III}, \theta)$, although they are not Gaussian. These two stochastic processes can then be combined with the Bayesian optimization for searching the global optima and for designing the training points in the epistemic uncertainty space.

The core of a Bayesian optimization method is the so-called learning function or acquisition as it determines the locations of the training points. Over the past several decades, many learning functions, which includes but not limited to, the expected improvement (EI) function, Probability of Improvement (PI) function, Knowledge Gradient(KG) function, Entropy Reduction (ER), Predictive Entropy Reduction (PER), etc., have been developed, and one can refer to Frazier (2018) for a review. The EI function is utilized in the work, but other learning functions also apply. There are also several versions of EI functions being established, and the one utilized in this work is formulated as:

$$L_*^{\mathrm{EI}}(x_{III}, \theta) = \mathbb{E}\left[\max\left(\mu_*(x_{III}^*, \theta^*) - \hat{*}(x_{III}, \theta), 0\right)\right] \tag{7}$$

In Eq.(7), $\mu_*(x_{III}^*, \theta^*)$ denotes the mean of variance or failure probability at site (x_{III}^*, θ^*), $\hat{*}(x_{III}, \theta)$ represents the corresponding stochastic process, and (x_{III}^*, θ^*) is the current best solution, which can be obtained by the following equation

$$(x_{III}^*, \theta^*) = \arg\min \mu_*(x_{III}, \theta) + \alpha \sigma_*(x_{III}, \theta) \tag{8}$$

with α measuring the degree of risk aversion, and the solutions of Eq.(8) are searched in the training set D

In practical application, Eq.(7) can not be calculated analytically as the distribution type and parameters of stochastic process $\hat{V}_y(x_{III},\theta)$ and $\hat{P}_f(x_{III},\theta)$ are unknown. A Monte Carlo simulation scheme is implied to estimate the above integration based on the random samples $\hat{V}_y^{(j)}$ and $\hat{P}_f^{(j)}$ of stochastic $\hat{V}_y$ and $\hat{P}_f$, by using of which, Eq.(7) can be estimated as

$$\hat{L}_*^{\mathrm{EI}}(x_{III},\theta) = \frac{1}{N_g}\sum_{j=1}^{N_g} \max\left(\hat{\mu}_*(x_{III}^*,\theta^*) - \hat{*}^{(j)}(x_{III},\theta),0\right) \tag{9}$$

where, the mean function $\mu_*(x_{III},\theta)$ and variance function $\sigma_*^2(x_{III},\theta)$ of $\hat{V}_y$ and $\hat{P}_f$ can be evaluated as

$$\begin{aligned}\hat{\mu}_*(x_{III},\theta) &= \frac{1}{N_g}\sum_{j=1}^{N_g}\hat{*}^{(j)}(x_{III},\theta)\\ \hat{\sigma}_*^2(x_{III},\theta) &= \frac{1}{N_g-1}\sum_{j=1}^{N_g}\left[\hat{*}^{(j)}(x_{III},\theta)-\mu_*(x_{III},\theta)\right]^2\end{aligned} \tag{10}$$

In Eq. 9 and 10, $\hat{*}^{(j)}(x_{III},\theta)$ refers to the j-th sample of the stochastic process $\hat{*}(x_{III},\theta)$, and will be discussed in detail in the following subsection.

The above MCS estimators will converges to the true values when the sample size approaches to infinity. By maximizing Eq.(9), a new design site $\left(x_{III}^+,\theta^+\right)$ will be solved, i.e.,

$$\left(x_{III}^+,\theta^+\right) = \arg\max \hat{L}_*^{\mathrm{EI}}(x_{III},\theta) \tag{11}$$

There are many global optimization algorithms, such as, particle swarm optimization, genetic algorithm, to solving Eq.(11).

In next subsection, an efficient sampling strategy is introduced to generate samples from the stochastic process $\hat{V}_y(x_{III},\theta)$ and $\hat{P}_f(x_{III},\theta)$.

3.3. Sampling strategy for Stochastic process

It is difficult to directly sample from $\hat{V}_y$ and $\hat{P}_f$ because the type of stochastic process and the distribution parameters are implicit. Then a indirectly way is implied by sampling from $\hat{\mathscr{G}}_D(\omega)$.

An efficient sampling procedure, named as "GPR conditioning sampling scheme", developed by Le Gratiet et al. (2014), is performed to sample from the posterior GPR model $\hat{\mathscr{G}}_D(\omega)$. Assume that $\hat{h}_D(\omega)$ follows a unconditional Gaussian process $\mathscr{GP}(0,\kappa(\omega,\omega'))$, then the posterior GPR model $\hat{\mathscr{G}}_D(\omega)$ can be rewritten as

$$\hat{\mathscr{G}}_D(\omega) = \mu_y(\omega) - \hat{\mu}_y(\omega) + \hat{h}_D(\omega) \tag{12}$$

with $\hat{\mu}_y(\omega)$ being

$$\hat{\mu}_y(\omega) = m(\omega) + \kappa(W,\omega)^{\mathbf{T}} K^{-1}\left(\hat{h}_D(W) - m(W)\right) \tag{13}$$

Based on the Eq.(12), the samples of $\hat{\mathscr{G}}_D(\omega)$ can be gained by sampling from the unconditional GP model $\hat{h}_D(\omega)$ using, such as, Karhunen-Loève (KL) expansion or stochastic harmonic function representation. In this work, the KL expansion is utilized to generate the samples of $\hat{h}_D(\omega)$. Let denoted by $\hat{\mathscr{G}}_D^{(j)}(\omega)$ with $j=1,\cdots,N_g$ the samples of $\hat{\mathscr{G}}_D(\omega)$ by using Eq.(12), where N_g is the size of the sample set.

Generate a set of joint samples $W = (X_I,U,X_{III},\mathscr{T})$ of size N_x. Once the samples set $\hat{\mathscr{G}}_D^{(j)}(\omega)$ is obtained, the samples $\hat{V}_y^{(j)}$ and $\hat{P}_f^{(j)}$ of stochastic $\hat{V}_y$ and $\hat{P}_f$ can be deduced as

$$\hat{V}_y^{(j)}(x_{III},\theta) = \frac{1}{N_x-1}\sum_{i=1}^{N_x}\left[\begin{array}{c}\hat{\mathscr{G}}_D^{(j)}\left(X_I^{(i)},U^{(i)},x_{III},\theta\right) - \\ \frac{1}{N_x}\sum_{k=1}^{N_x}\hat{\mathscr{G}}_D^{(j)}\left(X_I^{(k)},U^{(k)},x_{III},\theta\right)\end{array}\right]^2 \tag{14}$$

and

$$\hat{P}_f^{(j)}(x_{III},\theta) = \frac{1}{N_x}\sum_{i=1}^{N_x}\left[\hat{\mathscr{G}}_D^{(j)}\left(X_I^{(i)},U^{(i)},x_{III},\theta\right)<0\right] \tag{15}$$

with $X_I^{(i)}$ and $U^{(i)}$ being the i-th row of X_I and U respectively.

3.4. The adaptive design strategy

By maximizing the learning function introduced in Subsection 3.2, the design site $\left(x_{III}^+,\theta^+\right)$ in epistemic uncertainty space is generated. To ensure the accuracy of the estimates of the output variance and the failure probability at the site $\left(x_{III}^+,\theta^+\right)$, two

extra acquisition functions are introduced respectively for adaptively generating new design site in the aleatory uncertainty space of x_{III} and u respectively.

For reducing the posterior variance $\sigma^2_{V_y}(x_{III},\theta)$ of the output variance, the acquisition function, named as Posterior Variance Contribution (PVC) function, is utilized (Wei et al. (2020)), which is formulate as

$$L^{\mathbf{PVC}}(x_I,u) = f_I(x_I)\times f_u(u)\times \int_{\mathbb{R}^{n_I+n_{II}}} \mathrm{cov}_y\left(w,w'\right) f_I\left(x'_I\right) f_u\left(u'\right)\mathrm{d}x'_I\mathrm{d}u' \tag{16}$$

where $f_u(u)$ is the probability density of uniform distribution in interval $[0,1]$. The value of PVC function measures the contribution of the posterior variance of $\hat{\mathscr{G}}_D(\omega)$ at site ω, and by adding the maximum of PVC function, the most reduction of the variance $\sigma^2_V(x_{III},\theta)$ can be achieved. The PVC function is estimated by MCS with estimator:

$$\hat{L}^{\mathbf{PVC}}(x_I,u) = f_I(x_I)\times f_u(u)\times \frac{1}{N_x}\sum_{i=1}^{N_x}\mathrm{cov}_y\left(\left(x_I,u,x^+_{III},\theta^+\right),\left(x_I^{(i)},u^{(i)},x^+_{III},\theta^+\right)\right) \tag{17}$$

The acquisition function for estimating failure probability utilized in this paper is the **U**-function, which is formulated as

$$\mathbf{U}(x_I,u) = \frac{|\,\hat{\mu}_y\left(x_I,u,x^+_{III},\theta^+\right)\,|}{\hat{\sigma}_y\left(x_I,u,x^+_{III},\theta^+\right)} \tag{18}$$

The value of the $\Phi(-\mathbf{U}(x_I,u))$ measures the probability of misjudging the sign of the estimate $\hat{\mu}_y\left(x_I,u,x^+_{III},\theta^+\right)$. Assume that the sign of $\hat{\mu}_y\left(x_I,u,x^+_{III},\theta^+\right)$ can be correctly determined if $\mathbf{U}(x_I,u)>2$, otherwise, find the minimum $\left(x_I^+,u^+\right)$ of $\mathbf{U}(x_I,u)$, and add $\omega^+=\left(x_I^+,u^+,x^+_{III},\theta^+\right)$ to the training data set and update the GPR model.

3.5. Summary of CABO

Based on the above discussion, the main steps of CABO for estimating the bounds of variance or failure probability are summarized with the pseudocode displayed as Algorithm 1.

Algorithm 1: CABO method for estimating the bounds of variance or failure probability

Input: Augmented g-function $\mathscr{G}(w)$, sample size N_x, N_g, N_0, stopping threshold Δ^{EI}, Δ^{COV}

Output: Bounds $\mu_*\left(x^+_{III},\theta^+\right)$ of variance or failure probability and its corresponding site $\left(x_I^+,u^+,x^+_{III},\theta^+\right)$.

```
Generate a set of joint samples W = (X_I, U, X_III, T) of size N_x by random sampling;
Create the initial training set D of size N_0 from sample pool W;
while (1=1) do
    Train or update the GPR model Ĝ_D(ω) based on training set D;
    Generate a set of N_g samples Ĝ_D^(j)(ω) for Ĝ_D(ω) with j = 1,···,N_g;
    Compute the design site (x_III^+, θ^+) by Eq. (11);
    Compute the design site (x_I^+, u^+) by maximizing Eq. (17) or minimizing Eq. (18);
    if L^EI(x_III^+, θ^+) < Δ^BPO and COV_*(x_III^+, θ^+) < Δ^COV then
        break while-do;
    else
        add ω^+ = (x_I^+, u^+, x_III^+, θ^+) and G(ω^+) to the training set D;
    end
end
```

Before running Algorithm 1, the value of N_x of the size of sample set $\mathbf{W}$ should satisfy that the maximum of COV of bounds of variance or failure probability is less than a given threshold, such as Δ^{COV}, the value of N_g of the size of sample set $\hat{h}_{\mathscr{D}}(\omega)$ is recommended to be chosen in $1000\sim 5000$ according to the property of $\mathscr{G}(\omega)$. As mentioned above, the stopping threshold Δ^{EI} and Δ^{COV} are selected from $[0.001,0.01]$ and $[0.01,0.05]$ respectively. Algorithm 1 is developed for the lower bounds of the output variance and the failure probability, but it also applies to the upper bounds.

4. BENCHMARKS

4.1. Illustrative example

Considering the following two g-functions:

$$\begin{aligned} g_1(x) &= x_1\left(x_2^2 + x_2 + \cos(\pi x_3) - 7\right) \\ g_2(x) &= 7 - (x_1 + x_3)^2 + x_2 \end{aligned} \tag{19}$$

For g_1-function, $x_1 \sim N(0,1)$, $x_2 \sim N(\mu,2)$ with $\mu \in [-1.3, 1.8]$, and $x_3 \in [-0.5, 1.3]$; For g_2-function, $x_1 \sim N(0,1)$, $x_2 \sim N(\mu,2)$ with $\mu \in [-2,1]$, and $x_3 \in [-1,2]$.

CABO is implemented to estimate the bounds of the output variance of g_1-function by setting the initial training size N_0 as 30, Δ^{EI} be 0.005, and Δ^{COV} be 0.01. The algorithm successfully converges to the global optima by adding 55 samples, the results are displayed in Figure 1 and Table 1, together with the reference solution being computed analytically. One can see from Figure 1, the CABO methods can well search the global optimal points in each iteration until the convergence condition is satisfied. Let's take the lower bound of variance as an example, the estimate of which estimated by CABO is 18.980 with the posterior COV being 0.06 indicating that the results shows high accuracy and robustness. The difference between the optimal points obtained by CABO and reference extreme points is a little bigger, it is probably because the sensitivity of the model variance to these parameters is lower in the area around the extreme points revealed in Figure 1.

Table 1: Results of evaluating the bounds of variance of the numerical example.

Method	Bounds	Estimates	Points	COVs (%)	NOF
Ref	Lower	19	(0,1.3028)	–	–
	Upper	54.56	(1,-0.5)	–	
CABO	Lower	18.98	(0.05,1.26)	0.06	82
	Upper	54.63	(1.02,-0.57)	0.01	

Then, the bounds of failure probability of g_2-function is evaluated by the CABO algorithm with $N_0 = 20$, $\Delta^{\mathrm{EI}} = 0.005$, and $\Delta^{\mathrm{COV}} = 0.01$, the corresponding results are displayed in Figure 2 and Table 2, together with the reference solutions computed with double-loop MCS procedure. As shown

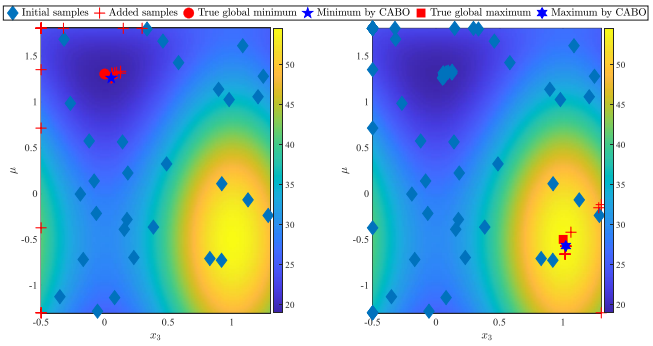

Figure 1: Training details in interval space of x_3 and μ of CABO for evaluating the bounds of output variance, with the heat map referring to the reference solution.

in Figure 2 and Table 2, the bounds of failure probability can be well estimate by CABO with high robustness. For the upper bound, the extreme points computed by CABO is as the same as the reference points, and the upper bound estimated by CABO shown high accuracy compared with the reference value. Though the lower bound is not well evaluated as the value of lower bound is too small to estimate using MCS, it does not affect the efficiency of the proposed method.

Table 2: Results of evaluating the bounds of failure probability of numerical example.

Method	Bounds	Means	Points	COVs (%)	NOF
Ref	Lower	0.0071	(-0.0264,1)	–	–
	Upper	0.4296	(2,-2)	–	
CABO	Lower	0.0076	(-0.0353,1)	0.50	29
	Upper	0.4203	(2,-2)	0.04	

5. CONCLUSIONS

An efficient framework named as CABO is proposed to estimate the bounds of variance and failure probability of a g-function with three category uncertainty inputs variables. The proposed method jointly perform Bayesian optimization in the epistemic parameter space and Bayesian cubature (or Bayesian reliability analysis) in the aleatory uncertainty space, and this way to adaptively produce training points in the joint space. The proposed is shown to be efficient and of good performance on global convergence. Results of the numerical example show that, bounds of both response

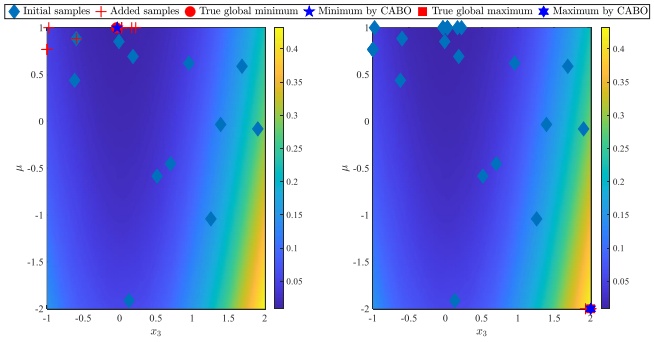

Figure 2: Training details in interval space of x_3 and μ of CABO for evaluating the bounds with the heat map referring to the reference solution of $P_f(x_3, \mu)$.

variance and failure probability are estimated with few training points, saving a lot of computational sources. It should be noted that, in some applications, the lower bound of the failure probability may be less accurately estimated, as its exact value is very small. For this case, advanced MCS methods, such as subset simulation needs to be properly embedded in the algorithm, and this will be conducted in the future work.

6. REFERENCES

Abdar, M., Pourpanah, F., Hussain, S., Rezazadegan, D., Liu, L., Ghavamzadeh, M., Fieguth, P., Cao, X., Khosravi, A., Acharya, U. R., et al. (2021). "A review of uncertainty quantification in deep learning: Techniques, applications and challenges." *Information Fusion*, 76, 243–297.

Abiodun, O. I., Jantan, A., Omolara, A. E., Dada, K. V., Mohamed, N. A., and Arshad, H. (2018). "State-of-the-art in artificial neural network applications: A survey." *Heliyon*, 4(11), e00938.

Beer, M., Ferson, S., and Kreinovich, V. (2013). "Imprecise probabilities in engineering analyses." *Mechanical Systems and Signal Processing*, 37(1-2), 4–29.

Chiles, J.-P. and Delfiner, P. (2009). *Geostatistics: modeling spatial uncertainty*, Vol. 497. John Wiley & Sons.

Crespo, L. G., Kenny, S. P., and Giesy, D. P. (2014). "The nasa langley multidisciplinary uncertainty quantification challenge." *16th AIAA Non-Deterministic Approaches Conference*, 1347.

Fox, J. and Okten, G. (2021). "Polynomial chaos as a control variate method." *SIAM Journal on Scientific Computing*, 43(3), A2268–A2294.

Frazier, P. I. (2018). "A tutorial on Bayesian optimization." *arXiv preprint arXiv:1807.02811*.

Hennig, P. and Schuler, C. J. (2012). "Entropy search for information-efficient global optimization." *The Journal of Machine Learning Research*, 13(1), 1809–1837.

Le Gratiet, L., Cannamela, C., and Iooss, B. (2014). "A bayesian approach for global sensitivity analysis of (multifidelity) computer codes." *SIAM/ASA Journal on Uncertainty Quantification*, 2(1), 336–363.

Patelli, E., Alvarez, D. A., Broggi, M., and Angelis, M. d. (2015). "Uncertainty management in multidisciplinary design of critical safety systems." *Journal of Aerospace Information Systems*, 12(1), 140–169.

Rasmussen, C. E. and Williams, C. (2006). "Gaussian processes for machine learning, vol. 1." *MIT press*, 39, 40–43.

Raychaudhuri, S. (2008). "Introduction to monte carlo simulation." *2008 Winter simulation conference*, IEEE, 91–100.

Wei, P., Hong, F., Phoon, K.-K., and Beer, M. (2021). "Bounds optimization of model response moments: a twin-engine bayesian active learning method." *Computational Mechanics*, 67(5), 1273–1292.

Wei, P., Lu, Z., and Song, J. (2014). "Extended monte carlo simulation for parametric global sensitivity analysis and optimization." *AIAA journal*, 52(4), 867–878.

Wei, P., Zhang, X., and Beer, M. (2020). "Adaptive experiment design for probabilistic integration." *Computer Methods in Applied Mechanics and Engineering*, 365, 113035.

Zhang, H., Dai, H., Beer, M., and Wang, W. (2013). "Structural reliability analysis on the basis of small samples: an interval quasi-monte carlo method." *Mechanical Systems and Signal Processing*, 37(1-2), 137–151.

Zhang, H., Mullen, R. L., and Muhanna, R. L. (2010). "Interval monte carlo methods for structural reliability." *Structural Safety*, 32(3), 183–190.